

Deviations from plastic barriers in $\text{Bi}_2\text{Sr}_2\text{CaCu}_2\text{O}_{8+\delta}$ thin films

Y. Z. Zhang, Z. Wang, X. F. Lu, and H. H. Wen

National Laboratory for Superconductivity, Institute of Physics and Center for Condensed Matter Physics,
Chinese Academy of Sciences, P.O. Box 603, Beijing, China

J. F. de Marneffe* and R. Deltour

Université Libre de Bruxelles, Physique des Solides, CP-233, B-1050, Brussels, Belgium

A. G. M. Jansen and P. Wyder

Grenoble High Magnetic Field Laboratory, Max-Planck-Institut für Festkörperforschung, and Centre National de la Recherche
Scientifique, 25, Avenue des Martyrs, Boîte Postale 166, F-38042 Grenoble Cedex 9, Grenoble, France

(Received 16 November 2004; published 16 February 2005)

Resistive transitions of an epitaxial $\text{Bi}_2\text{Sr}_2\text{CaCu}_2\text{O}_{8+\delta}$ thin film were measured in various magnetic fields ($\mathbf{H}\parallel\mathbf{c}$), ranging from 0 to 22.0 T. Rounded curvatures of low resistivity tails are observed in Arrhenius plot and considered to relate to deviations from plastic barriers. In order to characterize these deviations, an empirical barrier form is developed, which is found to be in good agreement with experimental data and coincide with the plastic barrier form in a limited magnetic field range. Using the plastic barrier predictions and the empirical barrier form, we successfully explain the observed deviations.

DOI: 10.1103/PhysRevB.71.052502

PACS number(s): 74.25.Fy, 74.25.Ha, 74.25.Qt

One of the most intriguing features of high- T_c superconductors (HTSCs) is the remarkable broadening of resistive transitions in applied magnetic fields. The broadening is related to thermal barriers (thermal activation energies) for vortex motion. In general, the vortex motion can be divided into three characteristic regimes.¹⁻⁵ In the high-temperature regime where the barrier $U_0 \leq T$, resistivity is given by flux flow resistivity $\rho \propto B/H_{c2}$. In the intermediate temperature regime, flux motion occurs through thermally assisted flux flow (TAFF), where flux lines are weakly pinned in the vortex liquid with $U_0 \gg T$, and resistivity $\rho \propto \exp(-U_0/T)$, where U_0 is independent of the current density j for $j \rightarrow 0$. In the low-temperature regime, the form $\rho \propto \exp(-U_0/T)$ remains valid for the resistivity analysis with $U_0(j)$ growing unlimitedly for $j \rightarrow 0$, thus leading to $\rho \rightarrow 0$.

$\text{Bi}_2\text{Sr}_2\text{CaCu}_2\text{O}_{8+\delta}$ (Bi-2212) is a strongly anisotropic superconductor with a layered crystalline structure. The corresponding vortex¹⁻³ matter is highly two-dimensional (2D) in high magnetic fields, and is 3D in low magnetic fields. The study of the activation energy of Bi-2212 is very interesting, as its TAFF regime is very broad and gives the necessary knowledge for understanding the vortex characteristics in HTSCs. Generally, resistivity in the TAFF regime is often analyzed in an Arrhenius plot with the approximation $\ln \rho(T, H) \approx \ln \rho_0 - U_0/T$,⁶ where $\ln \rho_0$ is the logarithmic resistivity for linearly extrapolating to $1/T=0$, and U_0 is the average slope for the resistivity data in the low resistivity portion of the curves. Palstra *et al.*⁶ found a power-law dependence $U_0 \propto H^{-\alpha}$ with ρ_0 being several orders magnitude larger than the normal state resistivity in HTSCs. Kucera *et al.*⁷ suggested that the prefactor ρ_0 could be highly reduced with a factor $\exp(U_0/T_c)$ and that the activation energy $U_0 \propto H^{-1/2}(1-T/T_c)$ for Bi-2212 thin films, where T_c was the critical temperature. The same relation $U_0 \propto H^{-1/2}(1-t)$ was also suggested by Wagner *et al.*⁸ for Bi-2212 thin films, where $t=T/T_c$.

For explaining the vortex dynamics of HTSCs, many theoretical approaches have been proposed to characterize the activation energies.^{1-6,9-11} Among these approaches, the scaling of the barrier $U \propto H^{-1/2}(1-t)$ was first theoretically suggested by Geshkenbein *et al.* in 1989,⁴ and then developed by Vinokur *et al.*⁵ This theory is based on the model of plastic flux creep ascribing the dissipation to the plastic shear of dislocations in a weakly pinned vortex liquid. It seems that this model perfectly describes the barrier relation of Bi-2212 thin films determined by Kucera *et al.*⁷ and Wagner *et al.*⁸ However, this model is based on the analysis of 3D vortex dynamics that provides a poor correspondence with the highly 2D vortex matter for which vortex cutting and reconnecting can change the plastic barriers in the same order of magnitude.⁵ Previously, most of the published papers have extensive discussions on the regions of validity of the plastic creep concept. Deviations of the concept in experiments are observed,^{6-8,12} but have not been studied detailedly until now. As a consequence, a detailed study of the creep deviations from the plastic barrier model predictions is of primary interest.

In this paper, we report measurements of resistive transitions of a Bi-2212 thin film in magnetic fields parallel to c axis from 0 to 22.0 T. Comparing these transitions with previously published papers, we develop an empirical barrier form for describing the deviations from plastic barriers. We find that this empirical form coincides with the plastic barrier form in a limited magnetic field range. By using this new expression, we successfully explain the observed deviations.

Epitaxial Bi-2212 thin films were prepared by an inverted cylinder magnetron sputtering technique on (100) SrTiO_3 and (100) LaAlO_3 substrates. The composition of the target was compensated in order to reach an ideal composition in the thin films. The sputtering gas was a 1:1 mixture of Ar and O_2 at 100 Pa. Deposition temperature was in the range of 810 °C–840 °C. After deposition, Bi-2212 thin films were

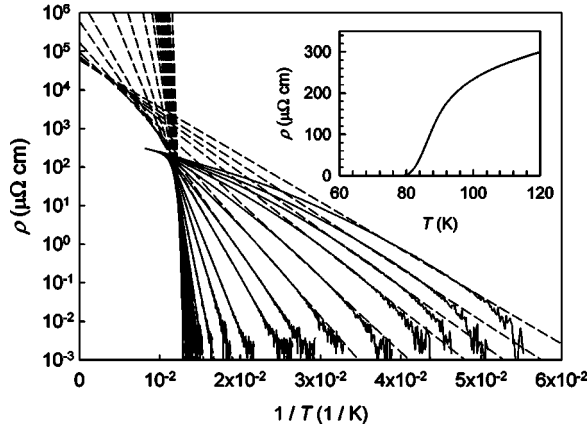


FIG. 1. The Arrhenius plot of the $\text{Bi}_2\text{Sr}_2\text{CaCu}_2\text{O}_{8+\delta}$ thin film. From left to right: $\mu_0 H = 0.0, 0.0037, 0.0052, 0.0070, 0.0089, 0.013, 0.021, 0.030, 0.050, 0.078, 0.113, 0.157, 0.302, 0.604, 1.0, 2.0, 3.0, 5.0, 8.0, 12.0, 15.0, 18.0, 22.0$ T. The dashed lines are linear regressions of the data in the range $10^{-4}\rho_n \leq \rho \leq 10^{-2}\rho_n$. The inset is the $\rho(T, H=0)$ curve.

annealed in an atmosphere of 10 Pa pure O_2 at ~ 500 °C for 45 min. X-ray diffraction patterns show that thin films are highly c -axis oriented and epitaxial. The studied film with a thickness of 210 ± 20 nm was patterned with a microbridge [$500 \mu\text{m}$ (length) \times $100 \mu\text{m}$ (width)]. Gold leads were stuck onto the film with silver paste. In order to reduce the resistance between the film and the gold wires, the film was baked at 350 °C in flowing oxygen for 6 h. Bipolar DC current of $40 \mu\text{A}$ (corresponding to the current density of $\sim 190 \text{ A/cm}^2$) was applied for the resistive measurement. This current density ensures that the low resistivity is ohmic in the most range for the measurement.⁸

Figure 1 shows $\rho(T, H)$ data of the Bi-2212 thin film in an Arrhenius plot. The dashed lines in Fig. 1 are linear regressions for the resistivity data range of $10^{-4}\rho_n \leq \rho \leq 10^{-2}\rho_n$, where $\rho_n = \rho(120 \text{ K}) \approx 300 \mu\Omega \text{ cm}$. A detailed examination of each curve suggests that these regressions are in good agreement with three or four order of magnitude of the resistivity data in a limited magnetic field range ($0.021 \leq \mu_0 H \leq 1.0$ T), but do only approximately average the rounded curvatures for the other ranges. In following discussion, we will simply use some special field values as just mentioned above, which are arbitrarily defined by the intended field values in measurements, as these values shall be close to the precise characteristic field values of the sample in reality and give very close information about the vortex matter.

Figure 2 shows $U_0(H)$ data. The linear regressions of $U_0(H)$ in the plot suggest a power-law dependence $U_0 \propto H^{-\alpha}$ with $\alpha \approx 0.258$ for $\mu_0 H \leq 0.113$ T, and $\alpha \approx 0.490$ for $\mu_0 H \geq 0.157$ T. The second α value consists with the plastic barrier form and the results determined in Refs. 7 and 8. However, rounded curvatures in the low resistivity portions are observed in the Arrhenius plot for $\mu_0 H < 0.021$ T and $\mu_0 H > 1.0$ T, which are apparently not described by the plastic barrier form.

Figure 3 shows the $\ln \rho_0(U_0)$ relation in both linear-linear and log-log scales. Note that $\ln \rho_0(U_0)$ is approximately lin-

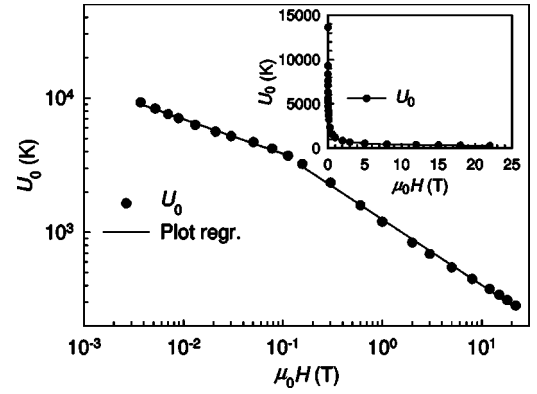


FIG. 2. Magnetic-field dependence of U_0 in both of the double log scale and the double linear scale (inset). The solid lines are plot regressions of U_0 for two different field regimes.

ear for $1190 < U_0 < 5620$ K corresponding to the field regime of $0.021 \leq \mu_0 H \leq 1.0$ T, where the regressions in the Arrhenius plots as shown in Fig. 1 are also linear, so that the determinations of $\ln \rho_0(U_0)$ are quite accurate through the regime, and can be assuredly used to deduce some important information as discussed below.

Considering the fact that many authors suggested $U_0 \propto (1-t)^\beta$ with $\beta=1$ in Refs. 4–8 and 13–15, $\beta=1.5$ in Refs. 6, 9, and 10, $\beta=2$ in Refs. 6 and 9, and the β value selected from 1.5 to 2.4 in Ref. 16, we start by assuming that $\rho = \rho_{0f} \exp[-U(T, H)/T]$, where ρ_{0f} is constant, $U(T, H) = g(H)f(t)$, g is the magnetic field dependence, $f = (1-t)^\beta$, and β accounts for the nonlinearity in the Arrhenius plot. Using the progression $(1-t)^\beta = 1 - \beta t + \beta(\beta-1)t^2/2! - \beta(\beta-1)(\beta-2)t^3/3! + \dots$, we obtain $\ln \rho \approx (\ln \rho_{0f} + g\beta/T_c) - (g/T)[1 + \beta(\beta-1)t^2/2! - \beta(\beta-1)(\beta-2)t^3/3! + \dots]$, where the term $(\ln \rho_{0f} + g\beta/T_c) \approx \ln \rho_0$ is temperature independent. With $\beta=1$, we have $\ln \rho_0 \approx \ln \rho_{0f} + U_0/T_c$ as observed in the linear part of Fig. 3 for $1190 < U_0 < 5620$ K (denoted by arrows), where $U_0 = g$. Here, the linear $\ln \rho(U_0)$ portion corresponds to the field range of $0.021 \leq \mu_0 H \leq 1.0$ T. By linearly extrapolating $\ln \rho_0(U_0)$ to $U_0=0$, we find that $\rho_{0f} \approx 69.7 \mu\Omega \text{ cm}$, and $T_c \approx 83.1$ K is the approximation of the inverse value of the slope in the double linear scale. Assum-

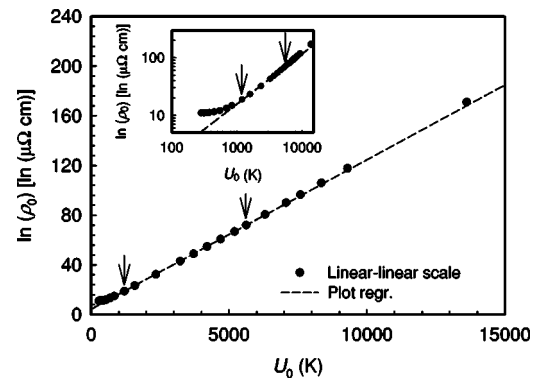


FIG. 3. $\ln \rho_0(U_0)$ data in both of the linear-linear scale and the log-log scale (inset). The dashed lines represent the plot linear regressions for $1190 < U_0 < 5620$ K (as denoted by the arrows).

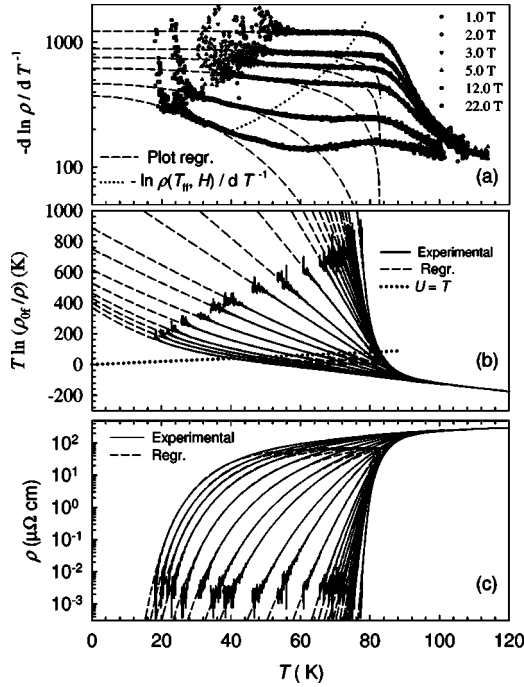


FIG. 4. (a) The different symbols give $-\partial \ln \rho / \partial T^{-1}$ data in several magnetic fields as denoted by corresponding symbols. The dotted line is the flux flow boundary determined in (b). (b) The solid lines present $U(T, H) \approx T \ln[\rho_{ff} / \rho(T, H)]$ data for all the tested magnetic fields. The dotted line is $U=T$ corresponding to the flux flow boundary. (c) The solid lines are $\rho(T, H)$ data for all the fields. The dashed lines in (a)–(c) are regressions using the empirical barrier form with the same $g(H)$ and $\beta(H)$ (see text).

ing $\beta = \text{const}$, a linear $\ln \rho_0(U_0)$ relation will be found. Obviously, $\beta = \text{const}$ (including $\beta = 1$) cannot account for the nonlinear portions of $\ln \rho_0(U_0)$ curves in the regimes of $U_0 < 1190$ K and $U_0 > 5620$ K. It is interesting to note that if β is magnetic field dependent, f becomes magnetic-field dependent, and thus a nonlinear character is introduced into the $\ln \rho_0(U_0)$ dependence.

Previously, a magnetic-field dependent f was proposed by Palstra *et al.*⁶ and Kim *et al.*¹⁶ by introducing a magnetic-field dependent $T_x(H)$ instead of T_c for the barrier scaling. Assuming $T_x = T_c / \beta$, we find $\ln \rho_0 \approx \ln \rho_{0f} + g / T_x$ for the similar explanation of the nonlinear $\ln \rho_0(U_0)$. In Bi-2212 thin films, Kucera *et al.*⁷ and Wagner *et al.*⁸ suggested that the barriers should scale according to $U \propto H^{-1/2}(1-t)$ with a constant T_c in t . However, $U(T, H)$ data for the low resistivity portion as mentioned by the authors in Fig. 4 of Ref. 7 do more favor $T_x(H)$ than T_c . Figure 4(a) shows $-\partial \ln \rho(T, H) / \partial T^{-1}$ data with different symbols for different magnetic fields. In the field range $0.021 \leq \mu_0 H \leq 1.0$ T (not all shown in the figure for clarity), the data are roughly temperature independent in the TAFF regime, indicating that $U \propto (1-t)$. Note that $f = 1-t$ will lead to $-\partial \ln \rho / \partial T^{-1} = U - T \partial U / \partial T = g$, where the g is temperature independent. For $\mu_0 H > 1$ T in the TAFF regime, $-\partial \ln \rho / \partial T^{-1}$ of our Bi-2212 thin film in Fig. 4(a) and Bi-2212 crystals in Ref. 6 are temperature dependent. It seems that similar temperature dependences can also be deduced from high-field data in Refs.

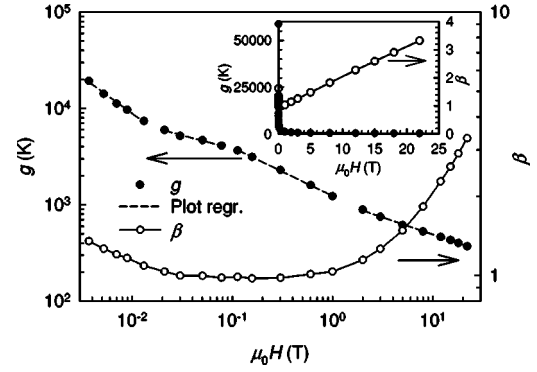


FIG. 5. Solid circles present $g(H)$ data and open circles show $\beta(H)$ data. The dashed lines correspond to the plot regressions in the log-log scale. The inset shows $g(H)$ and $\beta(H)$ data in linear-linear scales.

7 and 8. These temperature dependences do not support the $f = 1-t$ argument even by substituting $T_x(H)$ for T_c .

For high fields, each $-\partial \ln \rho / \partial T^{-1}$ monotonously decreases with temperature from low temperature to a local minimum. One may take the data around these minima for U simulation in which a constant β for $-\partial \ln \rho(T, H) / \partial T^{-1}$ data may be determined.^{17,18} However, taking into account the flux flow condition $U \leq T$, this may lead to a wrong result. Figure 4(b) shows $U(T, H) = T \ln[\rho_{ff} / \rho(T, H)]$ data with solid lines and the flux flow boundary $U=T$ with the dotted line. The flux flow temperature $T_{ff}(H)$ can be determined with the crossing points between the $U(T, H)$ lines and the dotted line $U=T$. We thus draw the flux flow boundary, $-\partial \ln \rho(T_{ff}, H) / \partial T^{-1}$, with a dotted line in Fig. 4(a). It is found that minima of $-\partial \ln \rho(T, H) / \partial T^{-1}$ may result in a corresponding temperature higher than T_{ff} for high fields. This means that the determination of a constant β around the minima of $-\partial \ln \rho(T, H) / \partial T^{-1}$ shall be dismissed.

As a result, we argue that we have to use $f = (1-t)^\beta$ as a substitute for $f = (1-t)$ in the barrier definition, where β is magnetic-field dependent. The dashed lines in Fig. 4(b) correspond to the best regressions using the expression $U(T, H) = g(1-t)^\beta$ for which the resistivity data in the range of $10^{-4} \rho_n \leq \rho \leq 10^{-2} \rho_n$ are used, where g and β are free fitting parameters. We also present dashed lines using the same $g(H)$ and $\beta(H)$ for $-\partial \ln \rho(T, H) / \partial T^{-1}$ and $\rho(T, H)$ in Figs. 4(a) and 4(c), respectively. These regressions are in good agreement with $U(T, H)$, $-\partial \ln \rho(T, H) / \partial T^{-1}$, and $\rho(T, H)$ in the TAFF regime.

Figure 5 shows $g(H)$ and $\beta(H)$ data, respectively. From the figure, we can roughly divide the g data into four magnetic field regimes according to the field values that were used in the measurements. We find that both $g(H)$ and $\beta(H)$ have an apparent increase for $\mu_0 H \leq 0.013$ T where $\alpha \approx 0.751$, and β increases with decreasing field, indicating a deviation from the plastic barrier model. As mentioned in many articles,^{19–21} the binding and unbinding behaviors of 2D vortex-antivortex pairs dominate the low resistivity in the low magnetic field range. Obviously, the 2D behaviors do not relate to the plastic vortex motion. In the range of $0.021 \leq \mu_0 H \leq 1.0$ T, $\beta \approx 1$, $\alpha \approx 0.275$ for $0.021 \leq \mu_0 H$

≤ 0.113 T, and $\alpha \approx 0.502$ for $0.157 \leq \mu_0 H \leq 1.0$ T. For $0.021 \leq \mu_0 H \leq 0.113$ T, the intervortex spacing is relatively large and the vortex matter is in a 3D state where the vortex system is very close to or can be in the plastic barrier regime.^{7,8} For $0.157 \leq \mu_0 H \leq 1.0$ T, both α and β have the values predicted by the plastic form, indicating that the vortex system is in the plastic barrier regime. Note that the vortex system changes from 3D to 2D at a crossover field $\mu_0 H_d \approx 4\phi_0/\gamma^2 d^2$, where γ is the anisotropic factor with $50 \leq \gamma \leq 200$ in Bi-2212,¹⁻³ d is the interplanar spacing, and ϕ_0 is the flux quantum. If $0.157 \leq \mu_0 H < \mu_0 H_d$, the vortex system is 3D for the plastic barriers. If $\mu_0 H_d < \mu_0 H < 1$ T, the system is in a 2D state where it maintains some 3D characteristics allowing plastic barrier behaviors. These 3D characteristics are gradually destroyed by further increasing the magnetic field ($\mu_0 H > 1.0$ T), where $\alpha \approx 0.355$ and β increases with $\mu_0 H$ as shown in Fig. 5. For $\mu_0 H > 1.0$ T, the vortex matter gradually crosses over into a highly 2D state where 2D vortices (pancake vortices) are largely overlapped and 2D collective interaction dominates the vortex behaviors; besides, the plastic vortex behavior has to fade away due to a strong interlayer decoupling.^{1-5,12} In particular, Kucera *et al.*⁷ and Wagner *et al.*⁸ also mentioned deviations of the plastic barriers at high magnetic fields which were suggested to relate to a 3D to 2D transition.

Note that both $U(T, H)$ and $-\partial \ln \rho(T, H)/\partial T^{-1}$ increase with decreasing temperature and deviate from the regressions in low temperature. This implies that the vortex coupling and pinning are enhanced. The deviations corresponding to the curvature differences and the curve separations between experimental data and fittings are a consequence of changes of competitive relations between pinning and depinning, and

between coupling (reconnecting) and decoupling (cutting). These changes may gradually drive $U(T, H)$ into the j dependent regime with decreasing temperature for $j \rightarrow 0$.

It is easily found that the barrier estimations with the empirical and the plastic barrier forms (g in Fig. 5 and U_0 in Fig. 2) have the same order that is just consistent with the plastic barrier prediction for any vortex deformation.⁵ In this case, the empirical form coincides with the plastic barrier prediction. The similar barrier relation and values, obtained by ac susceptibility measurements of a similar Bi-2212 thin film for $\mu_0 H \leq 1.0$ T, give a support to the $g(H)$ determination.²²

Note that the increasing β ($\beta > 1$) is a common behavior with increasing 2D feature for $\mu_0 H \leq 0.013$ T and $\mu_0 H > 1.0$ T. This implies that the increasing β features, as shown in Fig. 5, give the signs of a crossover from 3D to 2D, which differs on both field sides by its strength. For $H \rightarrow 0$, the low resistivity portion is dominated by the 2D behaviors of binding and unbinding of vortex-antivortex pairs. In high field, influences of interlayer decoupling and 2D collective behaviors must be taken into account for increasing H .

In summary, based on experimental results, we have developed an empirical barrier form $U \propto H^{-\alpha(H)}(1-t)^{\beta(H)}$ in Bi-2212 thin films. This expression coincides with the plastic barrier prediction over the magnetic-field range $0.021 \leq \mu_0 H \leq 1.0$ T, and can be applied to account for the deviations from plastic barriers in Bi-2212 thin films. Moreover, this model may possibly be used for the analysis of TAFF behaviors in other HTSCs.

This work was financially supported by the National Science Foundation of China (Grant Nos. 10174091 and 10174093).

*Present address: Interuniversitair Microelectronica Centrum—IMEC v.z.w., 75 Kapeldreef, B-3001 Leuven, Belgium.

¹G. Blatter, M. V. Feigel'man, V. B. Geshkenbein, A. I. Larkin, and V. M. Vinokur, *Rev. Mod. Phys.* **66**, 1125 (1994).

²E. H. Brandt, *Rep. Prog. Phys.* **58**, 1465 (1995).

³L. F. Cohen and H. J. Jensen, *Rep. Prog. Phys.* **60**, 1581 (1997).

⁴V. B. Geshkenbein, M. V. Feigel'man, A. I. Larkin, and V. M. Vinokur, *Physica C* **162**, 239 (1989).

⁵V. M. Vinokur, M. V. Feigel'man, V. B. Geshkenbein, and A. I. Larkin, *Phys. Rev. Lett.* **65**, 259 (1990); J. Kierfeld, H. Nordborg, and V. M. Vinokur, *ibid.* **85**, 4948 (2000).

⁶T. T. M. Palstra, B. Batlogg, R. B. van Dover, I. F. Schneemeyer, and J. V. Waszczak, *Phys. Rev. B* **41**, 6621 (1990).

⁷J. T. Kucera, T. P. Orlando, G. Virshup, and J. N. Eckstein, *Phys. Rev. B* **46**, 11 004 (1992).

⁸P. Wagner, F. Hillmer, U. Frey, and H. Adrian, *Phys. Rev. B* **49**, 13 184 (1994).

⁹Y. Yeshurun and A. P. Malozemoff, *Phys. Rev. Lett.* **60**, 2202 (1988).

¹⁰M. Tinkham, *Phys. Rev. Lett.* **61**, 1658 (1988).

¹¹M. V. Feigel'man and V. M. Vinokur, *Phys. Rev. B* **41**, 8986 (1990).

¹²Y. Z. Zhang, R. Deltour, and Z. X. Zhao, *Phys. Rev. Lett.* **87**,

209704 (2001); **85**, 3492 (2000); Y. Z. Zhang, R. Deltour, J. F. de Marneffe, H. H. Wen, Y. L. Qin, C. Dong, L. Li, and Z. X. Zhao, *Phys. Rev. B* **62**, 11 373 (2000).

¹³M. Andersson, A. Rydh, and Ö. Rapp, *Phys. Rev. B* **63**, 184511 (2001).

¹⁴D. Thopart, Ch. Goupil, and Ch. Simon, *Phys. Rev. B* **63**, 184504 (2001).

¹⁵J. Figueras, T. Puig, and X. Obradors, *Phys. Rev. B* **67**, 014503 (2003).

¹⁶D. H. Kim, K. E. Gray, R. T. Kampwirth, and D. M. McKay, *Phys. Rev. B* **42**, 6249 (1990).

¹⁷W. S. Kim, W. N. Kang, M. S. Kim, and S. I. Lee, *Phys. Rev. B* **61**, 11 317 (2000).

¹⁸T. Yang, Z. H. Wang, H. Zhang, Y. Nie, J. Fang, H. Luo, X. F. Wu, and S. Y. Ding, *Supercond. Sci. Technol.* **15**, 586 (2002).

¹⁹J. M. Kosterlitz and D. J. Thouless, *J. Phys. C* **6**, 1181 (1973).

²⁰B. I. Halperin and D. R. Nelson, *J. Low Temp. Phys.* **36**, 599 (1979).

²¹P. Minnhagen and P. Olsson, *Phys. Rev. Lett.* **67**, 1039 (1991); P. Minnhagen, *Phys. Rev. B* **44**, 7546 (1991); P. Minnhagen, and P. Olsson, *ibid.* **45**, 5722 (1992).

²²J.-F. de Marneffe, Y. Z. Zhang, and R. Deltour, *Physica C* **341-348**, 1165 (2000).